

AD-A136 435

LASER-INDUCED ELECTRON-PHONON PROCESSES ON METAL  
SURFACES(U) ROCHESTER UNIV NY DEPT OF CHEMISTRY  
W C MURPHY ET AL. DEC 83 UROCHESTER/DC/83/TR-46

1/1

UNCLASSIFIED

N00014-80-C-0472

F/G 7/5

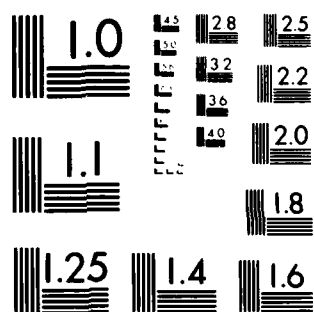
NL

END

DATE

FILED

DTIC



MICROCOPY RESOLUTION TEST CHART  
NATIONAL BUREAU OF STANDARDS-1963-A

AD-A136435

OFFICE OF NAVAL RESEARCH  
Contract N00014-80-C-0472  
Task No. NR 056-749  
TECHNICAL REPORT No. 46

Laser-Induced Electron-Phonon  
Processes on Metal Surfaces

by

William C. Murphy and Thomas F. George

Prepared for Publication

in

Journal of Chemical Physics

Department of Chemistry  
University of Rochester  
Rochester, New York 14627

DTIC  
C D  
DEC 30 1983  
H

December 1983

Reproduction in whole or in part is permitted for any  
purpose of the United States Government.

This document has been approved for public release  
and sale; its distribution is unlimited.

DTIC FILE COPY

83 12 30 003

Unclassified

SECURITY CLASSIFICATION OF THIS PAGE (When Data Entered)

REPORT DOCUMENTATION PAGE		READ INSTRUCTIONS BEFORE COMPLETING FORM
1. REPORT NUMBER UROCHESTER/DC/83/TR-46	2. GOVT ACCESSION NO.	3. RECIPIENT'S CATALOG NUMBER
4. TITLE (and Subtitle) Laser-Induced Electron-Phonon Processes on Metal Surfaces		5. TYPE OF REPORT & PERIOD COVERED
		6. PERFORMING ORG. REPORT NUMBER
7. AUTHOR(s) William C. Murphy and <u>Thomas F. Goerge</u>		8. CONTRACT OR GRANT NUMBER(s) N00014-80-C-0472
9. PERFORMING ORGANIZATION NAME AND ADDRESS Department of Chemistry University of Rochester Rochester, New York 14627		10. PROGRAM ELEMENT, PROJECT, TASK AREA & WORK UNIT NUMBERS NR 056-749
11. CONTROLLING OFFICE NAME AND ADDRESS Office of Naval Research Chemistry Program Code 472 Arlington, Virginia 22217		12. REPORT DATE December 1983
		13. NUMBER OF PAGES 22
14. MONITORING AGENCY NAME & ADDRESS (if different from Controlling Office)		15. SECURITY CLASS. (of this report) Unclassified
		15a. DECLASSIFICATION DOWNGRADING SCHEDULE
16. DISTRIBUTION STATEMENT (of this Report) This document has been approved for public release and sale; its distribution is unlimited.		
17. DISTRIBUTION STATEMENT (of the abstract entered in Block 20, if different from Report)		
18. SUPPLEMENTARY NOTES  Prepared for publication in Journal of Chemical Physics		
19. KEY WORDS (Continue on reverse side if necessary and identify by block number) ELECTRON-PHONON PROCESSES      EXCITATION OF SURFACE STATES SECOND-ORDER PERTURBATION THEORY      SODIUM METAL SURFACES      ONE-DIMENSIONAL MODEL LASER-INDUCED      LOWER CROSS SECTION THAN FOR SILICON		
20. ABSTRACT (Continue on reverse side if necessary and identify by block number) Electronic charge transfer from bulk to surface states in metals induced by laser radiation is examined. Due to the position of the Fermi energy, it is necessary to also include phonon excitations. Cross sections for this second-order process are presented. Comparison with the surface excitation in semiconductors is made. It is seen that for metals the required laser frequencies are larger and the cross sections substantially less than for semiconductors. ←		

DD FORM 1 JAN 73 1473

Unclassified

SECURITY CLASSIFICATION OF THIS PAGE (When Data Entered)

LASER-INDUCED ELECTRON-PHONON PROCESSES ON METAL SURFACES

William C. Murphy and Thomas F. George

Department of Chemistry  
University of Rochester  
Rochester, New York 14627  
USA

Electronic charge transfer from bulk to surface states in metals induced by laser radiation is examined. Due to the position of the Fermi energy, it is necessary to also include phonon excitations. Cross sections for this second-order process are presented. Comparison with the surface excitation in semiconductors is made. It is seen that for metals the required laser frequencies are larger and the cross sections substantially less than for semiconductors.



Accession For	
NTIS GRA&I	<input checked="checked" type="checkbox"/>
DTIC TAB	<input type="checkbox"/>
Unannounced	<input type="checkbox"/>
Justification	
By _____	
Distribution/	
Availability Codes	
A1	

## I. Introduction

In a previous paper [1], we examined the effects of laser radiation on the surface states of a semiconductor. Within a one-dimensional model, the optical cross section was calculated for the excitation of electrons from the bulk valence band to various surface states. For surface states with charge densities confined to the first few lattice layers, a large cross section on the order of  $1$  or  $2 \text{ \AA}^2$  was discovered. This indicated that a low-power laser ( $1\text{-}10 \text{ W/cm}^2$ ) could be used effectively to transfer charge from the bulk of the crystal to the surface region. Furthermore, this surface charge was shown to have a significant influence on the interaction with a charged adspecies [2]. Consequently, we suggested that this effect could be used to enhance the desorption or adsorption of charged or polar atoms and molecules.

In the above studies, we confined our efforts to examining wide-band semiconductors. However, metals have a band structure that is qualitatively similar to the energy levels of these semiconductors. Consequently, we would expect that laser radiation could also be used to transfer charge to metal surfaces and thus influence surface dynamics.

In Section II we shall show that our one-dimensional model developed for semiconductors can easily be extended to the case of metals. In Section III we shall use time-dependent perturbation theory to examine surface excitations. This theory involves electron-phonon coupling, which will be evaluated in Section IV. In Section V the optical cross sections at various laser frequencies for the metals will be presented.

Finally, in Section VI we shall discuss the differences with our previous works and suggest possible ways to enhance the laser-stimulated surface dynamics in metals.

## II. The Model

As with wide-band semiconductors, the valence electron wave functions of a metal of infinite extent can be written as a sum of plane waves [3]. Consequently, if we model a metal as a truncated one-dimensional chain, the bulk wave function,  $\psi_k(z)$  obtained via the nearly-free-electron approximation will be functionally the same for a metal and a semiconductor:

$$\psi_k(z) = \left\{ 1 + \left[ \frac{E_k - \frac{k^2}{2}}{V_g} \right]^2 \right\}^{-\frac{1}{2}} \left\{ \phi_k(z) + \frac{E_k - \frac{k^2}{2}}{V_g} \phi_{k-g}(z) \right\}, \quad (1)$$

where for  $z < a/2$

$$\phi_k(z) = \left(\frac{2}{L}\right)^{1/2} \sin[k(z - \frac{a}{2}) + \theta_k], \quad (2A)$$

and for  $z > a/2$

$$\phi_k(z) = \left(\frac{2}{L}\right)^{1/2} \sin\theta_k e^{-q_k(z - \frac{a}{2})}. \quad (2B)$$

$L$  is the length of the chain,  $a$  is the lattice constant,  $g$  is the reciprocal lattice vector,  $k$  is the electron wave vector, and  $V_g$  is the lattice interaction matrix. The phase factor and the exponential constant are given elsewhere [4]. This wave function has the corresponding energy

$$E_k = \frac{1}{4} \{ [k^2 + (k-g)^2] \pm \sqrt{[k^2 - (k-g)^2]^2 + 4E_g^2} \}, \quad (3)$$

where  $E_g$  is the band gap.

To obtain the wave function for the surface states, we assume the wave vectors to be complex,

$$k = \frac{g}{2} + i\kappa \quad (4)$$

but the energies to be real [5]. Consequently, some algebra [4] leads to the surface wave functions

$$\psi_\kappa(z) = C_s \sin\left[\left(\frac{g}{2}\right)\left(z - \frac{a}{2}\right) + \theta_\kappa\right] e^{-\kappa\left(z - \frac{a}{2}\right)} \quad (5A)$$

for  $z < a/2$  and

$$\psi_\kappa(z) = C_s \sin\theta_\kappa e^{-q_\kappa\left(z - \frac{a}{2}\right)} \quad (5B)$$

for  $z > a/2$ , where the normalization constant, the phase factor and the exponential constant are found elsewhere [4]. The corresponding energy is

$$E_\kappa = \frac{1}{2} \left[ \left(\frac{g}{2}\right)^2 - \kappa^2 \pm \sqrt{E_g^2 - \kappa^2 g^2} \right]. \quad (6)$$

The dispersion relation, given by eqs. (3) and (6), is illustrated in Fig. 1. As can be seen the band structure is similar to that of the semiconductor previously calculated [1]. However, whereas in the semiconductor the lower band was populated to the top, in a metal the Fermi energy,  $E_F$ , lies somewhat below. For example, in the case of sodium the



Fermi energy is 0.7 eV below the band edge and, thus, the surface states. This immediately implies that our laser frequency must be higher in metals than in semiconductors in order to excite electrons to the surface states. To calculate this laser-induced transition rate between the bulk states, eq. (1), and the surface states, eq. (5), we proceed as previously by examining the coupling between these states via time-dependent perturbation theory.

### III. Perturbation Theory

If the metal is now exposed to laser radiation in order to excite bulk states to surface states, it will be seen that the transitions that conserve the real part of the crystal momentum are favored. This selection rule was previously developed for semiconductors [1,4] and is still valid for metals since our wavefunctions, eqs. (1) and (5), are essentially the same. However, there are no occupied bulk states with real momentum at or near  $g/2$  which is the real momentum of the surface states [eq. (4)]. To overcome this problem, the electrons can be excited not only with a laser but also with the vibrational momentum of the crystal. Thus, photons would supply the energy needed for the transition and phonons would supply the needed crystal momentum. A suggested pathway for this combined photon and phonon excitations is illustrated in Fig. 1

For the one-dimensional model, the electronic Schrödinger equation is

$$i \frac{\partial \psi(z,t)}{\partial t} = H(t) \psi(z,t) \quad (7)$$

where

$$H(t) = H^0 + H^f e^{-i\omega_f t} + H^p e^{-i\omega_p t}. \quad (8)$$

$H^0$  is the electronic Hamiltonian of the system in the ground state,  $H^f$  is the coupling of electrons to the laser field of frequency  $\omega_f$ , and  $H^p$  is the coupling of the electrons to a phonon of frequency  $\omega_p$ . Our wave function is expanded in terms of the stationary states:

$$\psi(z,t) = |k''; n_K\rangle e^{-iE_k t} + \sum_k C_k |k; n_K-1\rangle e^{-iE_k t} \quad (9)$$

where  $k$  in the ket notation refers to the stationary electronic states, eq. (1) and (5), and  $n_K$  refers to the phonon number state with crystal momentum  $K$ . The double prime refers to an electronic state below the Fermi energy, and no prime labels a surface state.

If first-order perturbation theory is now applied, we obtain

$$\begin{aligned} i \dot{C}_k^{(1)} = & \langle k; n_K-1 | H^f | k''; n_K \rangle e^{i[E_k - E_{k''} - \omega_f]t} \\ & + \langle k; n_K-1 | H^p | k''; n_K \rangle e^{i[E_k - E_{k''} - \omega_p]t}. \end{aligned} \quad (10)$$

However, the first term will vanish since the laser field is not coupled to the phonons, and thus crystal momentum is not conserved. The second term is also zero since one phonon term cannot supply sufficient energy for the excitation. Consequently, higher-order perturbation theory must be used [6].

In second-order perturbation theory, the electron is first excited to an intermediate state and then to the final state:

$$|k''; n_K\rangle \xrightarrow{\omega_p} |k'; n_K-1\rangle \xrightarrow{\omega_f} |k; n_K-1\rangle, \quad (11)$$

where the initial state  $k''$  below the Fermi energy is excited by absorption of a phonon to intermediate state  $k'$  in the same band and from there excited to the final surface state  $k$  by a photon. This pathway is illustrated in Fig. 1. Another possible pathway is

$$|k''; n_K\rangle \xrightarrow{\omega_f} |k'; n_K\rangle \xrightarrow{\omega_p} |k; n_K-1\rangle. \quad (12)$$

Here the first excitation is done by the photon, and the intermediate state  $k'$  will lie in an upper conduction band. Because of the large energy mismatch in each step, however, this pathway would contribute only a small part to the transition rate. Consequently, only the first pathway, eq. (11), is considered.

Second-order perturbation theory will now yield

$$C_k^{(2)} = \sum_{k'} \frac{H_{kk'}^f H_{k'k''}^p}{\omega_{k'k''} - \omega_p} \left[ \frac{e^{i(\omega_{kk''} - \omega_p - \omega_f)t} - 1}{\omega_{kk''} - \omega_p - \omega_f} \right] \quad (13)$$

where

$$H_{kk'}^f = \langle k; n_K-1 | H^f | k'; n_K-1 \rangle, \quad (14)$$

$$H_{k',k''}^D = \langle k'; n_k - 1 | H^D | k''; n_k \rangle, \quad (15)$$

and

$$\omega_{kk''} = E_k - E_{k''}. \quad (16)$$

We have only considered the conservative term and disregarded that due to the sudden turning on of the perturbation [7]. Taking the modulus squared of eq. (13) at large times, we obtain the transition rate from state  $k''$ :

$$\lim_{t \rightarrow \infty} \frac{C_k C_k^*}{t} = 2\pi \left( \sum_{k'} \frac{H_{kk', H_{k', k''}^D}}{\omega_{k', k''} - \omega_p} \right)^2 \delta(\omega_{kk''} - \omega_p - \omega_f), \quad (17)$$

where  $\delta(\dots)$  is the Dirac delta function. To proceed further and calculate the total transition rate, we must first determine an expression for  $H^D$ , as done below.

#### IV. Electron-Phonon Coupling

The total lattice potential,  $V(z)$ , can be written as a sum of ionic potentials

$$V(z) = \sum_{\ell} v(z - Z_{\ell}), \quad (18)$$

where  $v(z - Z_{\ell})$  is the screened potential caused by the lattice ion at position  $Z_{\ell}$ . If a single phonon is present we, can write

$$Z_\ell = Z_\ell^0 + U_\ell e^{-i\omega_p t}, \quad (19)$$

where  $Z_\ell^0$  is the ionic equilibrium position and  $U_\ell$  is the displacement amplitude.

Using a Taylor series, we obtain

$$V(z) = V^0(z) + \sum_\ell v'(z - Z_\ell^0) U_\ell e^{-i\omega_p t}, \quad (20)$$

where  $v'(z - Z_\ell^0)$  is the gradient of the screened potential evaluated at equilibrium.  $V^0(z)$  is the equilibrium potential that is contained in  $H^0$  [eq. (8)]. The second term is due to the electron-phonon coupling, and thus

$$H_{k',k}^D = \langle k'; n_k - 1 | v'(z - Z_\ell^0) U_\ell | k''; n_k \rangle. \quad (21)$$

It is convenient to express the displacement in terms of the phonon annihilation,  $a(K)$ , and creation  $a^\dagger(K)$ , operators [8]:

$$U_\ell = [2NM \omega_p]^{-\frac{1}{2}} [e^{iKZ_\ell} a(K) + e^{-iKZ_\ell} a^\dagger(K)], \quad (22)$$

where  $M$  is the mass of the lattice atoms and  $N$  is the total number of these atoms. Using eq. (22) in eq. (21), we obtain

$$H_{k',k}^D = \sum_\ell [2NM \omega_p]^{-\frac{1}{2}} e^{iKZ_\ell} n_K^{1/2} \langle k' | v'(z - Z_\ell^0) | k'' \rangle. \quad (23)$$

To evaluate the integral in this expression, we note that the bulk stationary states in a metal can be roughly approximated by a plane wave:

$$|k\rangle = \frac{1}{L^{1/2}} e^{ikz}. \quad (24)$$

Consequently, eq. (23) becomes

$$H_{k'k''}^p = -i(NM)^{-1/2} \frac{v(k'-k'')}{[2\omega_p]^{1/2}} n_{k'-k''}^{1/2} \delta_{K,k'-k''}, \quad (25)$$

where  $v(k'-k'')$  is the Fourier transform of  $v(z)$  and  $\delta_{K,k'-k''}$  is the Kronecker delta function. Eq. (25) constitutes the electron-phonon coupling in our transition, which will now be combined with the field coupling to yield the optical cross section below.

#### V. Cross Sections

Using eq. (25), we can readily simplify eq. (17) to give

$$\lim_{t \rightarrow \infty} \frac{C_k C_k^*}{t} = \left( \frac{\pi}{NM} \right) \delta(\omega_{kk''} - \omega_p - \omega_f) \sum_{k'} \frac{H_{kk'}^2 (k'-k'')^2 v(k'-k'')^2 n_{k'-k''}^{1/2} \delta_{K,k'-k''}}{(\omega_{k'k''} - \omega_p)^2 \omega_p}. \quad (26)$$

To find the total transition rate,  $T$ , we must sum over all possible initial,  $k''$ , final,  $k$ , and phonon,  $K$ , states:

$$T = \sum_k \sum_{k''} \sum_K \lim_{t \rightarrow \infty} \frac{C_k C_k^*}{t}. \quad (27)$$

To simplify the transition rate, we make use of our previously determined field coupling [1,4]:

$$(H_{\kappa k'}^f)^2 = \left(\frac{2\pi I}{137}\right) \frac{g}{\omega_f} \delta(k' - \frac{g}{2}) \frac{|\langle \kappa | \frac{d}{dz} | k' \rangle|_0^2}{1 - e^{2\kappa a}}, \quad (28)$$

where  $I$  is the intensity of the laser and the subscript zero implies integration over the first unit cell. Furthermore, since only the imaginary part of the surface state wave vector changes [see eq. 4], we have replaced the index  $k$  with  $\kappa$ .

Defining the optical cross section by

$$\sigma \equiv \frac{\omega I}{I} \quad (29)$$

and using eqs. (26), (27) and (28), we obtain

$$\sigma = \frac{1}{N} \sum_K \frac{K^2 v^2(K) n_K}{2M(\omega_{g/2, g/2-K} - \omega_p)^2 \omega_p} \sigma^{(1)}(\kappa), \quad (30)$$

where  $\sigma^{(1)}(\kappa)$  has the same functional form as the cross section previously obtained from first-order perturbation theory [1,4]. The phonon wave vector,  $\kappa$ , and the complex part of the surface wave vector,  $\kappa$ , are related by the resonance condition

$$\omega_f + \omega_p = E_{\kappa} - E_{g/2-K}. \quad (31)$$

The first-order cross section term multiplied by the field frequency is plotted in Fig. 2 using parameters characterized of sodium [9].

The zero near the center of the plot is due to the branch point in the energy, eq. (6), at which there is no surface state. The cross section diverges at the high-energy side, because at this point one should be considering absorption coefficients for transitions between bulk bands. It should also be noted that  $\omega_{f\sigma}^{(1)}(\kappa)$  is independent of field frequency.

In view of eq. (30), all phonon effects can be grouped into a scaling factor:

$$S(K) \equiv \frac{\kappa^2 v^2(K) n_K}{2M \omega_p (\omega_{g/2, g/2-K} - \omega_p)^2} \quad (32)$$

The phonon states in this one-dimensional system are given by the dispersion relation [3]

$$\omega_p = \omega_{\max} \sin\left(\frac{\kappa a}{2}\right), \quad (33)$$

where  $\omega_{\max}$  is the maximum frequency of the acoustic phonons. The population of the phonon states is assumed to be thermal and thus given by the Bose-Einstein statistics,

$$n_K = \frac{1}{e^{\beta \omega_p} - 1}, \quad (34)$$

where  $\beta$  is the Boltzmann factor. Using eqs. (33) and (34) in eq. (32) along with the potential  $v(K)$  given by Appapillari and Williams [10], we have obtained the scaling factor for sodium at room temperature and show our results in Fig. 3. The exponential shape of the curve



is due to the domination of the population term, eq. (34), in the scaling expression. This curve is also independent of any laser present or any initial or final states. It depends only on the phonon wave vector  $K$ .

If we now wished to obtain the total cross section, eq. (30) would be written in the form

$$\sigma = \frac{1}{N} \sum_K S(K) \sigma^{(1)}(\kappa). \quad (35)$$

However, it is not clear over which states the sum should be performed. If one sums over over all possible phonon states, for instance, surface states near the band edge would be included. Since these states have a great deal of bulk character, they are of little interest in surface dynamics but they would dominate the total cross section. Furthermore, to understand how charge is transferred to the surface, it is more instructive to look at the "cross sections",  $\sigma_\kappa$ , for individual surface states:

$$\sigma_\kappa \equiv S(K) \sigma^{(1)}(\kappa), \quad (36)$$

where again  $K$  and  $\kappa$  are related by eq. (31). Again, using parameters for sodium,  $\sigma_\kappa$  is plotted in Fig. 4 for a variety of laser frequencies from the infrared (0.925 eV) to the ultraviolet (4.213 eV). Laser frequencies which are less than the difference between the band edge and the Fermi energy,  $\Delta$ , are too small to excite surface states. On the other hand, if the laser frequency is greater than  $E_F + \Delta + E_g$ , the photons will be too large to excite surface states. Results for other laser frequencies can readily be obtained by combining

values of  $\sigma^{(1)}(\kappa)$ , Fig. 2, and  $S(K)$ , Fig. 3, under the appropriate resonance condition, eq. (31).

## VI. Discussion

The second-order cross section, Fig. 4, is readily comparable with the cross sections previously obtained for a semiconductor [1]. However, whereas the scale for the semiconductor cross section was in  $\text{\AA}^2$ , the results for surface excitations in metals are smaller by a factor of  $10^{-4}$ . This means that a larger laser power ( $10\text{--}100 \text{ KW/cm}^2$ , in contrast to  $1\text{--}10 \text{ W/cm}^2$ ) would be needed in the metal to achieve a similar surface excitation.

In silicon, the laser frequency needed to achieve surface excitation is between 0.0 eV and 1.2 eV. In sodium the frequency is between 0.7 eV and 4.4 eV. Hence, the metal requires a much higher frequency for surface excitation, but offers a broader range of frequencies from which to choose.

Furthermore, in a semiconductor one could be selective in the surface state excited: one laser frequency would only excite one surface state. However, in a metal, any given laser frequency would excite a number of surface states, and the total cross section would be a sum of these excitations, eq. (30). Certain groups of surface states nonetheless would be more favored than others in a metal for a given laser frequency (see Fig. 4).

Since our goal is to increase surface charge in order to effect surface dynamics, as in the semiconductor, the main surface states of interest lie near the center of the gap, roughly between  $0.4 E_g$  and  $0.6 E_g$ . This confines the surface charge to the first 5 or 6 layers

of the lattice. Because one laser frequency in a metal excites several surface states, this would tend to enhance the surface charge more than in a semiconductor where only one state is excited. The surface charge could be further increased by heating the surface and thus increasing the supply of phonons [see eq. (32)].

In the foregoing discussion, the laser was used to excite the electrons while the phonons were thermally excited. A more detailed model of surface excitation should consider the possible coupling of the same laser or a different laser to the surface phonons. Such phonon excitations would increase the optical cross section and would improve the selectivity of the electronic excitation. Furthermore, the presence of adspecies on the surface can alter both the electron and phonon dispersion relation. Such alterations could enhance the surface charge excitation. Finally, the effects of higher dimensionality must be considered for a more realistic description of the laser surface excitation. These and other problems associated with laser-stimulated surface dynamics are the subject of continuing research.

#### Acknowledgements

This research was supported by the Air Force Office of Scientific Research (AFCS), United States Air Force, under Grant AFOSR-82-0046, the Office of Naval Research and the U.S. Army Research Office. The United States Government is authorized to reproduce and distribute reprints for governmental purposes notwithstanding any copyright notation hereon. TFG acknowledges the Camille and Henry Dreyfus Foundation for a Teacher-Scholar Award (1975-84) and the John Simon Guggenheim Memorial Foundation for a Fellowship (1983-84).

### References

1. W. C. Murphy and T. F. George, Surface Sci. 114 (1982) 189.
2. W. C. Murphy and T. F. George, J. Phys. Chem. 86 (1982) 4481.
3. J. M. Ziman, Principles of the Theory of Solids (Cambridge Press, London, 1964), p. 31, p. 74 ff.
4. T. F. George, J. Lin, A. C. Beri and W. C. Murphy, Prog. Surf. Sci., in press.
5. S. Lundqvist, in Surface Science, Vol. 1 (International Atomic Energy Agency, Vienna, 1975) p. 331.
6. W. C. Murphy, A. C. Beri, T. F. George and J. Lin in Laser Diagnostics and Photochemical Processing for Semiconductor Devices, ed. by R. M. Osgood, Jr. and S. R. J. Brueck (Elsevier, New York), Mat. Res. Soc. Symp. Proc. 17, 273 (1983).
7. L. I. Schiff, Quantum Mechanics (McGraw-Hill, New York, 1955) p. 201.
8. J. Callaway, Quantum Theory of the Solid State (Academic Press, New York, 1976) p. 576 ff.
9. C. Kittel, Introduction to Solid State Physics, 4th Ed. (Wiley, New York, 1971) pp. 38, 364, 338.
10. N. Appapillai and A. R. Williams, J. Phys. F 3 (1973) 759.

### Figure Captions

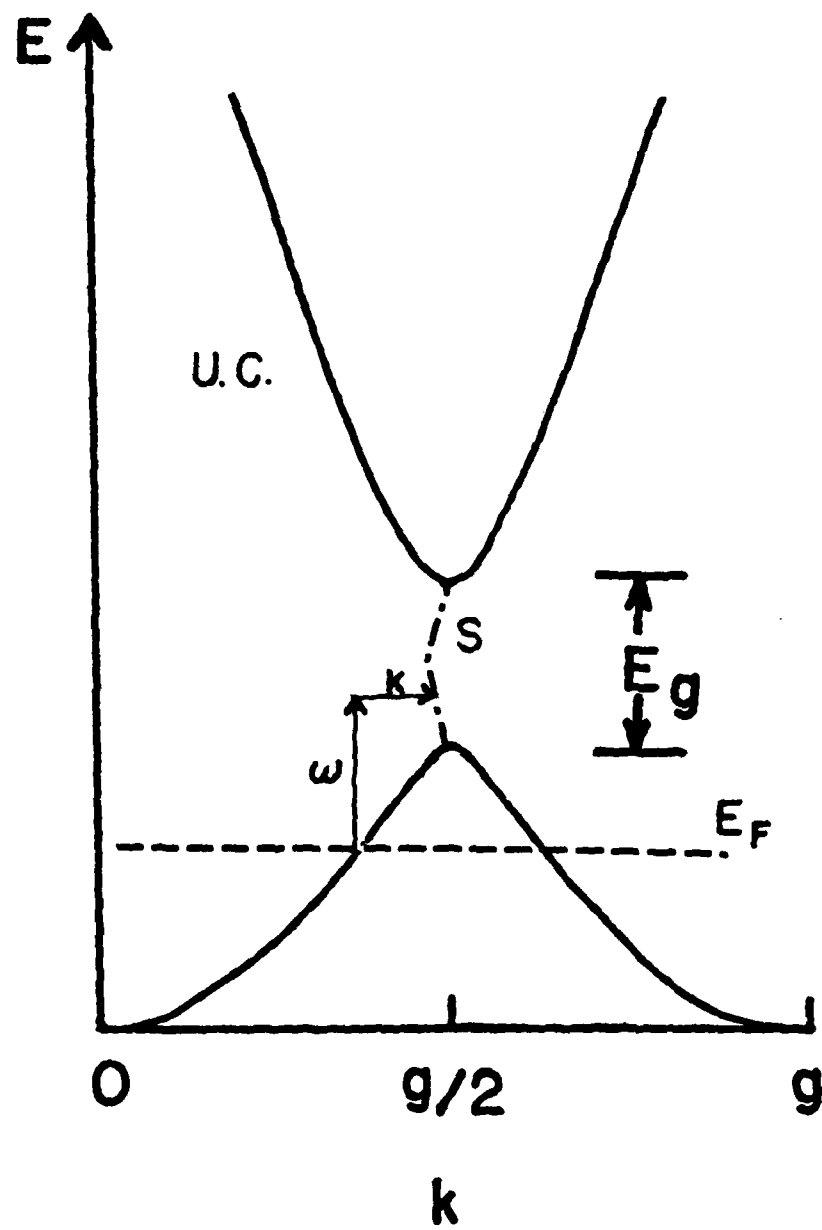
Fig. 1. Dispersion relation for a metal and an excitation pathway to the surface states. The vertical arrow represents a photon of frequency  $\omega$ ; the horizontal arrow, a phonon of momentum  $K$ . UC is an upper conduction band. The dot-dash line is the projection of the surface states on the  $(E \text{ versus real } k)\text{-plane}$ .

Fig. 2. Laser field frequency multiplied by the first-order cross section in units of  $10^{-2} \text{ ha}_0^2$  versus the energy of the surface state measured from the band edge.

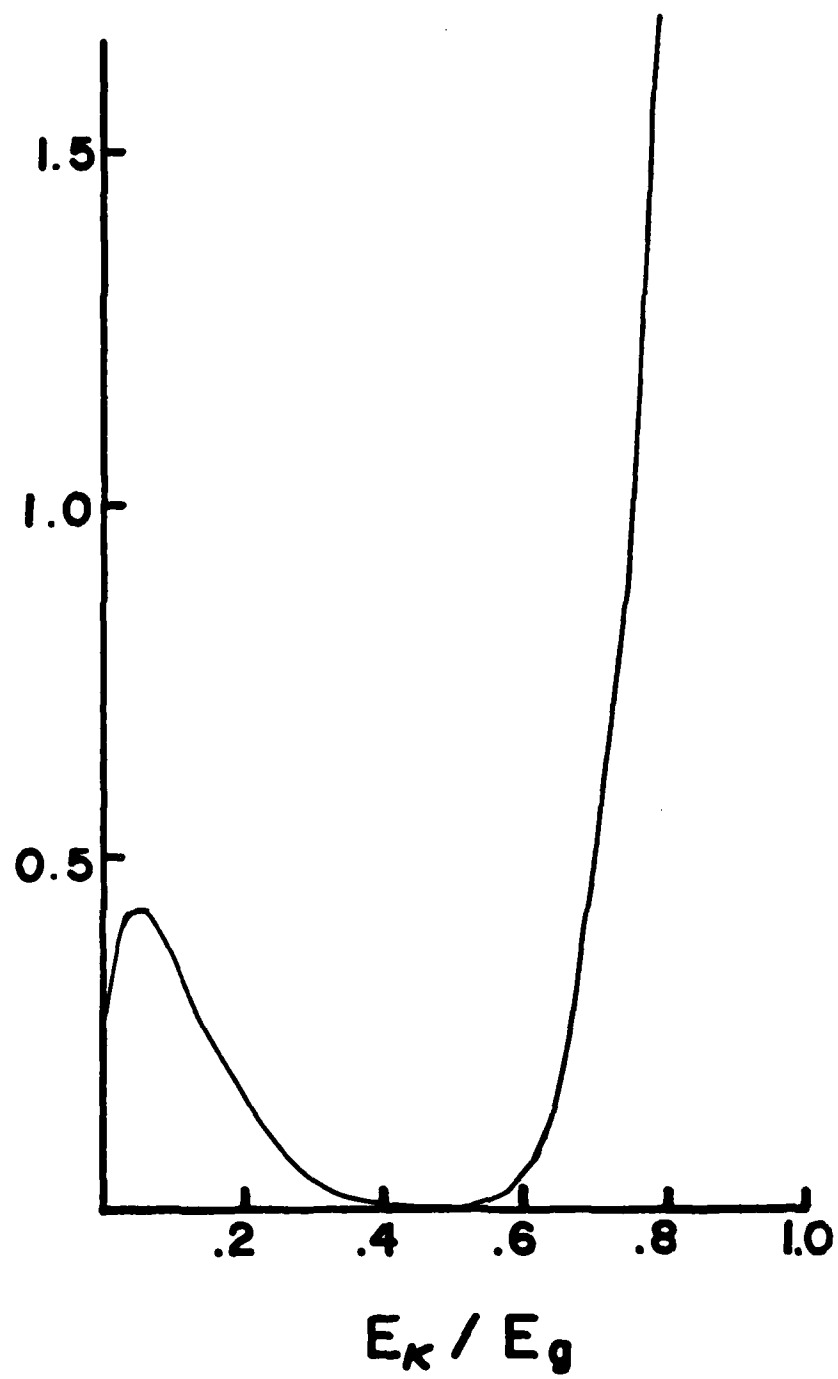
Fig. 3. Phonon scaling factor versus the phonon wave vector.

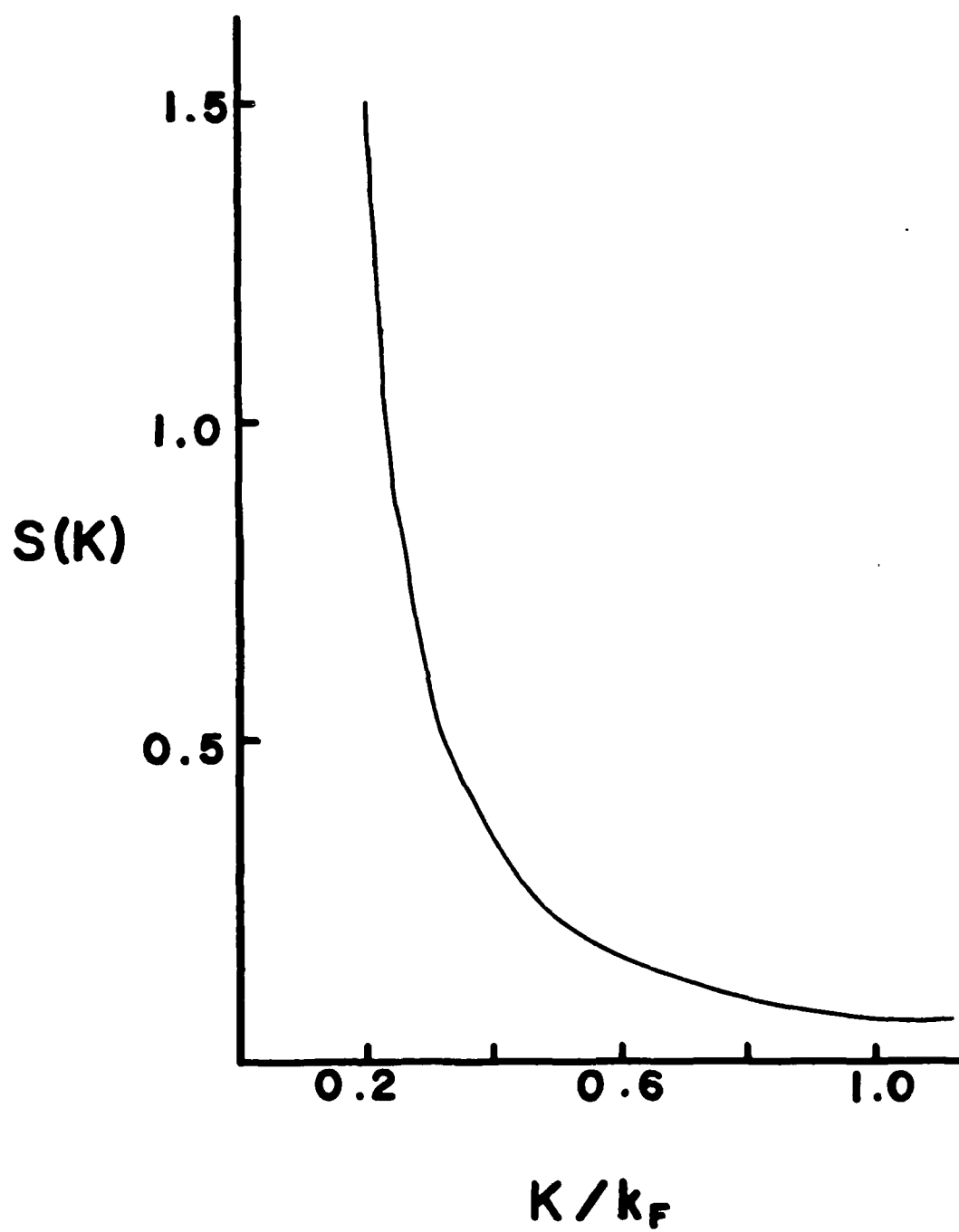
Fig. 4. Cross sections for surface state  $\kappa$  in units of  $\text{pm}^2$  versus the energy of the surface state measured from the band edge. Curve (1) has  $\omega_f = \Delta + \frac{E_g}{2}$  (0.925 eV); (2)  $\omega_f = \Delta + E_g$  (1.150 eV); (3)  $\omega_f = \frac{E_f + E_g + 2\Delta}{2}$  (2.569 eV); (4)  $\omega_f = E_F + \Delta$  (3.988 eV); and (5)  $\omega_f = E_F + \Delta + \frac{E_g}{2}$ .

Fig. 1 JSP  
M. J. P. ...

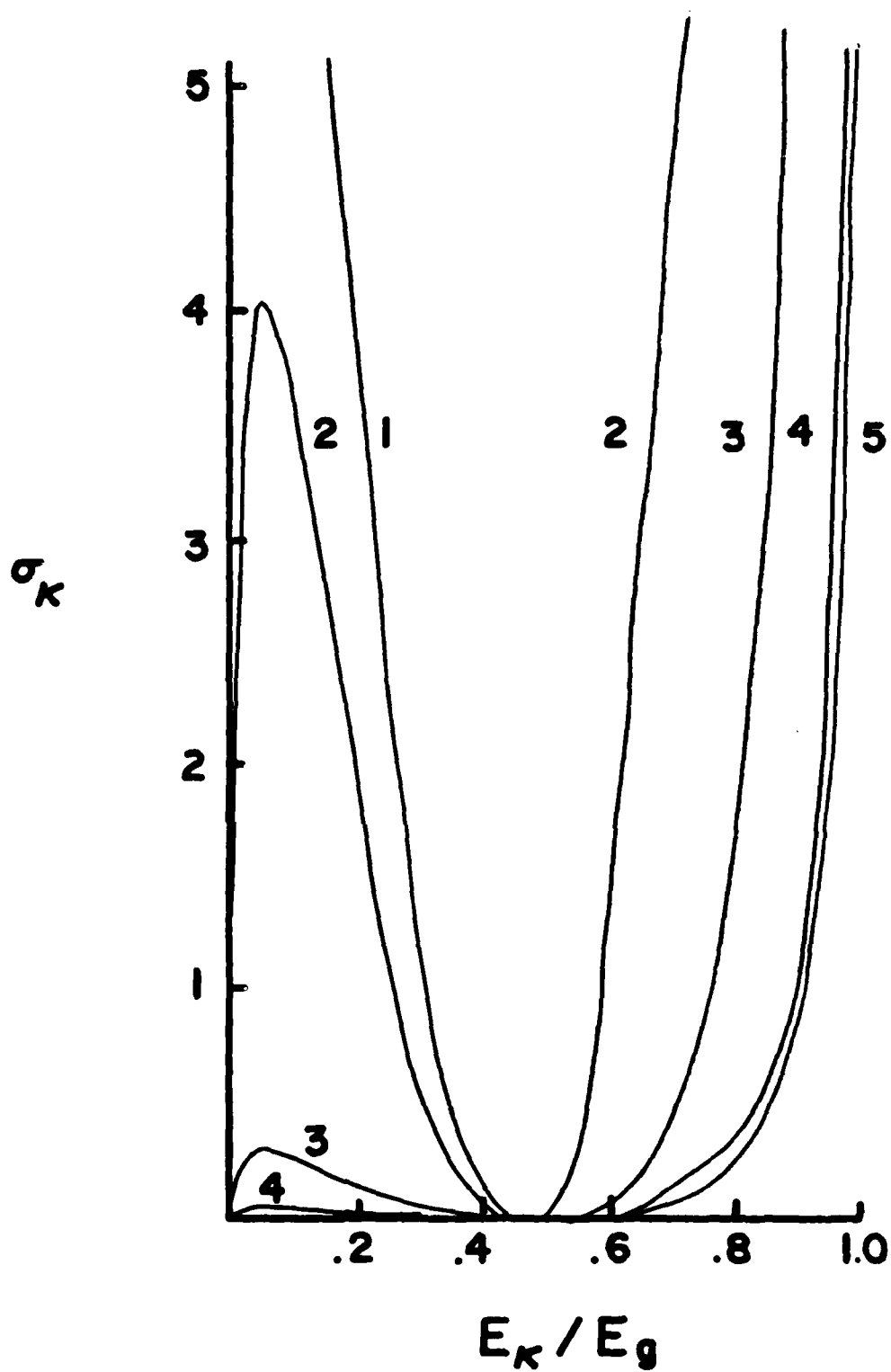


$\omega_f \sigma_K^{(1)}$









TECHNICAL REPORT DISTRIBUTION LIST, GEN

	<u>No. Copies</u>		<u>No. Copies</u>
Office of Naval Research Attn: Code 413 800 N. Quincy Street Arlington, Virginia 22217	2	Naval Ocean Systems Center Attn: Technical Library San Diego, California 92152	1
ONR Pasadena Detachment Attn: Dr. R. J. Marcus 1030 East Green Street Pasadena, California 91106	1	Naval Weapons Center Attn: Dr. A. B. Amster Chemistry Division China Lake, California 93555	1
Commander, Naval Air Systems Command Attn: Code 310C (H. Rosenwasser) Washington, D.C. 20360	1	Scientific Advisor Commandant of the Marine Corps Code RD-1 Washington, D.C. 20380	1
Naval Civil Engineering Laboratory Attn: Dr. R. W. Drisko Port Hueneme, California 93401	1	Dean William Tolles Naval Postgraduate School Monterey, California 93940	1
Superintendent Chemistry Division, Code 6100 Naval Research Laboratory Washington, D.C. 20375	1	U.S. Army Research Office Attn: CRD-AA-IP P.O. Box 12211 Research Triangle Park, NC 27709	1
Defense Technical Information Center Building 5, Cameron Station Alexandria, Virginia 22314	12	Mr. Vincent Schaper DTNSRDC Code 2830 Annapolis, Maryland 21402	1
DTNSRDC Attn: Dr. G. Bosmajian Applied Chemistry Division Annapolis, Maryland 21401	1	Mr. John Boyle Materials Branch Naval Ship Engineering Center Philadelphia, Pennsylvania 19112	1
Naval Ocean Systems Center Attn: Dr. S. Yamamoto Marine Sciences Division San Diego, California 91232	1	Mr. A. M. Anzalone Administrative Librarian PLASTEC/ARRADCOM Bldg 3401 Dover, New Jersey 07801	1
Dr. David L. Nelson Chemistry Program Office of Naval Research 800 North Quincy Street Arlington, Virginia 22217	1		

TECHNICAL REPORT DISTRIBUTION LIST, 056

Dr. G. A. Somorjai  
Department of Chemistry  
University of California  
Berkeley, California 94720

Dr. J. Murday  
Naval Research Laboratory  
Surface Chemistry Division (6170)  
455 Overlook Avenue, S.W.  
Washington, D.C. 20375

Dr. J. B. Hudson  
Materials Division  
Rensselaer Polytechnic Institute  
Troy, New York 12181

Dr. Theodore E. Madey  
Surface Chemistry Section  
Department of Commerce  
National Bureau of Standards  
Washington, D.C. 20234

Dr. Chia-wei Woo  
Department of Physics  
Northwestern University  
Evanston, Illinois 60201

Dr. Robert M. Hexter  
Department of Chemistry  
University of Minnesota  
Minneapolis, Minnesota

Dr. J. E. Demuth  
IBM Corporation  
Thomas J. Watson Research Center  
P.O. Box 218  
Yorktown Heights, New York 10598

Dr. M. G. Lagally  
Department of Metallurgical  
and Mining Engineering  
University of Wisconsin  
Madison, Wisconsin 53706

Dr. Adolph B. Amster  
Chemistry Division  
Naval Weapons Center  
China Lake, California 93555

Dr. W. Kohn  
Department of Physics  
University of California, San Diego  
La Jolla, California 92037

Dr. R. L. Park  
Director, Center of Materials  
Research  
University of Maryland  
College Park, Maryland 20742

Dr. W. T. Peria  
Electrical Engineering Department  
University of Minnesota  
Minneapolis, Minnesota 55455

Dr. Keith H. Johnson  
Department of Metallurgy and  
Materials Science  
Massachusetts Institute of Technology  
Cambridge, Massachusetts 02139

Dr. J. M. White  
Department of Chemistry  
University of Texas  
Austin, Texas 78712

Dr. R. P. Van Duyne  
Chemistry Department  
Northwestern University  
Evanston, Illinois 60201

Dr. S. Sibener  
Department of Chemistry  
James Franck Institute  
5640 Ellis Avenue  
Chicago, Illinois 60637

Dr. Arold Green  
Quantum Surface Dynamics Branch  
Code 3817  
Naval Weapons Center  
China Lake, California 93555

Dr. S. L. Bernasek  
Princeton University  
Department of Chemistry  
Princeton, New Jersey 08544

TECHNICAL REPORT DISTRIBUTION LIST, 056

Dr. F. Carter  
Code 6132  
Naval Research Laboratory  
Washington, D.C. 20375

Dr. Richard Colton  
Code 6112  
Naval Research Laboratory  
Washington, D.C. 20375

Dr. Dan Pierce  
National Bureau of Standards  
Optical Physics Division  
Washington, D.C. 20234

Professor R. Stanley Williams  
Department of Chemistry  
University of California  
Los Angeles, California 90024

Dr. R. P. Messmer  
Materials Characterization Lab.  
General Electric Company  
Schenectady, New York 22217  
12301

Dr. Robert Gomer  
Department of Chemistry  
James Franck Institute  
5640 Ellis Avenue  
Chicago, Illinois 60637

Dr. Ronald Lee  
R301  
Naval Surface Weapons Center  
White Oak  
Silver Spring, Maryland 20910

Dr. Paul Schoen  
Code 5570  
Naval Research Laboratory  
Washington, D.C. 20375

Dr. John T. Yates  
Department of Chemistry  
University of Pittsburgh  
Pittsburgh, Pennsylvania 15260

Dr. Richard Greene  
Code 5230  
Naval Research Laboratory  
Washington, D.C. 20375

Dr. L. Kesmodel  
Department of Physics  
Indiana University  
Bloomington, Indiana 47403

Dr. K. C. Janda  
California Institute of Technology  
Division of Chemistry and Chemical  
Engineering  
Pasadena, California 91125

Professor E. A. Irene  
Department of Chemistry  
University of North Carolina  
Chapel Hill, North Carolina 27514

Dr. Adam Heller  
Bell Laboratories  
Murray Hill, New Jersey 07974

Dr. Martin Fleischmann  
Department of Chemistry  
Southampton University  
Southampton SO9 5NH  
Hampshire, England

Dr. John W. Wilkins  
Cornell University  
Laboratory of Atomic and  
Solid State Physics  
Ithaca, New York 14853

Dr. Richard Smardzewski  
Code 6130  
Naval Research Laboratory  
Washington, D.C. 20375

TECHNICAL REPORT DISTRIBUTION LIST, 056

Dr. R. G. Wallis  
Department of Physics  
University of California  
Irvine, California 92664

Dr. D. Ramaker  
Chemistry Department  
George Washington University  
Washington, D.C. 20052

Dr. P. Hansma  
Physics Department  
University of California  
Santa Barbara, California 93106

Dr. J. C. Hemminger  
Chemistry Department  
University of California  
Irvine, California 92717

Professor T. F. George  
Chemistry Department  
University of Rochester  
Rochester, New York 14627

Dr. G. Rubloff  
IBM  
Thomas J. Watson Research Center  
P.O. Box 218  
Yorktown Heights, New York 10598

Professor Horia Metiu  
Chemistry Department  
University of California  
Santa Barbara, California 93106

Captain Lee Myers  
AFOSR/NC  
Bolling AFB  
Washington, D.C. 20332

Professor Roald Hoffmann  
Department of Chemistry  
Cornell University  
Ithaca, New York 14853

Dr. R. W. Plummer  
Department of Physics  
University of Pennsylvania  
Philadelphia, Pennsylvania 19104

Dr. E. Yeager  
Department of Chemistry  
Case Western Reserve University  
Cleveland, Ohio 44106

Professor D. Hercules  
University Pittsburgh  
Chemistry Department  
Pittsburgh, Pennsylvania 15260

Professor N. Winograd  
Department of Chemistry  
Pennsylvania State University  
University Park, Pennsylvania 16802

Dr. G. D. Stein  
Mechanical Engineering Department  
Northwestern University  
Evanston, Illinois 60201

Professor A. Steckl  
Department of Electrical and  
Systems Engineering  
Rensselaer Polytechnic Institute  
Troy, New York 12181

Professor G. H. Morrison  
Department of Chemistry  
Cornell University  
Ithaca, New York 14853

Dr. David Squire  
Army Research Office  
P.O. Box 12211  
Research Triangle Park, NC 27709

